Articles

Tenuous Structures from Disorderly Growth Processes

T. A. WITTEN AND M. E. CATES

Colloidal aggregation and other random growth processes produce structures that behave differently from ordinary bulk matter. Much of this behavior can be described in terms of the invariance of the aggregates under changes of spatial length scale: they appear to be fractals. There are two types of basic mechanisms for producing fractal aggregates. Those in which aggregation proceeds cluster by cluster can be understood qualitatively in terms of a solvable schematic model. The diffusion-limited aggregation or deposition of individual particles to make a large cluster is not as well understood. It is closely related to several irreversible processes in other areas of physics, such as two-fluid displacement in porous materials and the dielectric breakdown of insulators. More generally, disorderly growth mechanisms provide structures having unique properties, many of which can be understood by using simple statistical principles.

An electron micrograph of a typical colloidal aggregate is shown in Fig. 1 (*1*). Such an aggregate is made in aqueous solution from a dilute mist of individual gold particles about 100 Å in diameter. The gold particles are initially formed with a net electric charge; their mutual repulsion keeps them dispersed in the water. However, if the reagent pyridine is added, it neutralizes this charge, and the particles are then attracted to one another by van der Waals forces. Since the spheres are many atoms in size, this attraction energy is much larger than an average thermal energy; thus, the particles stick almost irreversibly on contact. Because particles in solution undergo random (Brownian) motion, a period occurs during which the neutralized gold particles collide at random and stick to make small clusters. These clusters also collide (with single particles or with other clusters) to make larger ones. After minutes or hours, the particles have flocculated to form large, wispy, treelike aggregates such as the one shown in two-dimensional projection in Fig. 1.

Aggregates like this occur widely in nature and in technology. An example is soot (carbon black), which is formed as a by-product of combustion and is found in diesel exhausts (*2*). Aggregated carbon black, when incorporated into a rubber matrix, forms a tough elastic compound that is used to make tires (*3*). Similar aggregates made of silica particles are used as fluid additives (*4*); a small percentage (by weight) of such material added to a liquid such as paint can thicken it and help to control its rate of flow. The flocculation of colloids, which leads to precipitation of low-density, finely divided solids, provides an important means of chemical separation (for example, of mineral ores) and purification (for example, of drinking water) (*5*). In nature, the properties of tenuous aggregated materials may determine the mechanical properties of a snow pack or the efficiency of a blood clot.

Another disorderly growth process is shown in Fig. 2. This fingering pattern is produced when a highly viscous fluid (such as oil) is displaced from a porous material (such as sandstone) as a less viscous fluid (such as water) is pumped in (*6–9*). The water tends to flow along threadlike fingers through the oil instead of displacing it in a pistonlike fashion. This tendency poses a major obstacle to attempts to push oil out of the ground by displacing it with water. One way of understanding viscous fingering is in terms of an equivalent aggregation process. Further examples are the closely related patterns that arise from dendritic solidification and electrodeposition (*10–13*), such as the mossy deposits that form on the terminals of a car battery, and from the dielectric breakdown of an insulator in a high electric field (*14*).

The structure of random aggregates has fascinated researchers for many years (*15–18*). It is now believed that the apparently formless complexity in Figs. 1 and 2 embodies a subtle type of regularity, called dilation symmetry, or spatial scale invariance (*19–22*).

Properties of Scale-Invariant Structures

A scale-invariant structure, or fractal (*23*), is an object whose statistical properties are unchanged under a dilation, or change of spatial length scale. In other words, two pieces of a fractal, one of size ℓ and the other of a smaller size ℓ', are statistically equivalent over some wide range of intermediate lengths, as long as the smaller piece is enlarged by a factor ℓ/ℓ'.

The distribution of gaps, or white areas, on the micrograph of Fig. 1 suggests that the cluster is a fractal. There is a hierarchy of smaller and smaller gaps extending down from the scale of the entire cluster to the scale of a single particle. Between these two extremes, there is no typical length scale for gaps, nor for any other feature of the cluster geometry. The absence of a characteristic length indicates dilation symmetry.

One finds quantitative evidence for this symmetry by drawing a sphere of radius R around an arbitrary point on the cluster and counting the number of particles, $N(R)$, lying within that sphere. On average

$$N(R) \sim R^D \tag{1}$$

where D is about 1.7 (*1*). The same value of D appears under a variety of experimental conditions and for radii R ranging from about the size of a particle to about that of the whole cluster. The

T. A. Witten is a research associate and M. E. Cates is a postdoctoral research fellow at Corporate Research Science Laboratories, Exxon Research and Engineering Company, Annandale, NJ 08801. This article is based in part on a lecture published in (*20*), pages 212 to 230.

simple power-law behavior is the only form allowed by dilation symmetry. The parameter D varies from one type of fractal to another; it is called the fractal dimension. This term arises by extension from the familiar examples of one-, two-, and three-dimensional materials (straight lines, smooth surfaces, and uniform solid objects), which are described by Eq. 1 with D equal to 1, 2, and 3, respectively. From Eq. 1 one sees that the average density of particles, $\rho \sim N(R)/R^d$, within a fractal of size R varies as R^{D-d}, where d is the number of dimensions of the physical space that contains the fractal ($d = 3$ or 2). Evidently, D is no greater than d, otherwise ρ would increase indefinitely as R increases. For fractals of $D < d$, as in Fig. 1, the average density becomes arbitrarily small as R increases. Hence these fractals are inherently tenuous, sparsely connected objects, that span large regions of empty space.

It is often helpful to imagine a fractal object embedded in a space of more than three dimensions ($d > 3$). (Just as three-dimensional space can be thought of as a stack of two-dimensional spaces—that is, planes—a four-dimensional space can be imagined as a stack of three-dimensional spaces, and so on.) Some aggregation processes become very simple to understand when they occur in an imagined space of many dimensions.

A well-studied example of a fractal is the random-walk trajectory of a diffusing particle. It is well known that for such a walk of N steps, the average distance traveled varies as $R \sim N^{1/2}$. Thus, by comparison with Eq. 1, we see that $D = 2$ for this structure. Random walks in higher space dimensions also have $D = 2$. Many other well-studied examples of fractals arise in equilibrium statistical mechanics (*24–27*). A distinguishing feature of the aggregates discussed in this article is that they are formed by irreversible processes and consequently are not in equilibrium. Nonetheless, evidence from theoretical work (*28, 29*), computer simulations (*30–33*), and experiments (*1, 7–9, 11–14, 34–37*) shows that these aggregates are fractals, with values of D between 1.5 and 2.5.

Another important simplification in the description of aggregates is that they appear to be treelike, that is, they have essentially no large loops (*28–37*). (This is not obvious from the projected view in Fig. 1.) Suppose we measure the length $L(r)$ of the (single) connecting path along the aggregate between two points on it at spatial separation r. We expect to find, on average

$$L(r) \sim r^{\delta} \tag{2}$$

Again, this simple power-law dependence is the only form consistent with dilation symmetry. For the random walk mentioned above, $\delta = 2$. The exponent δ complements D by providing information about the geometry of a treelike fractal aggregate: the larger δ is, the more tortuous the pathway between any two points. From δ one can predict how transport processes, such as electrical conduction or the diffusion of a particle, are modified when constrained to take place on the structure (*38–42*). Another unusual property of a fractal aggregate, which also depends on δ, is its elastic behavior (*43, 44*). As the size of an aggregate increases, it becomes less and less rigid, ultimately attaining a floppy state in which the branches are completely flexible beyond a certain length (*44–46*).

Fractal aggregates modify external phenomena in the surrounding space in a characteristic way. A conducting fractal modifies the electric field around it; an adsorbing fractal modifies the local concentration of a diffusing species; and a fractal immersed in fluid modifies the surrounding flow. The basic laws governing these external processes can be expressed solely in terms of the fractal dimension D. As an example, we consider the interaction of a fractal aggregate with a ray of light. We imagine a tiny light source somewhere in the middle of the fractal and ask what is the probability that it will be visible from a given point outside. This is simply unity minus the probability that the light ray from the source to our eye intersects the aggregate. A similar problem concerns the escape of a diffusing particle, or random walker, from an absorbing cluster. If the particle is released from the interior of the cluster, its probability of escape is unity minus the probability of intersection between the cluster and an infinitely long random walk.

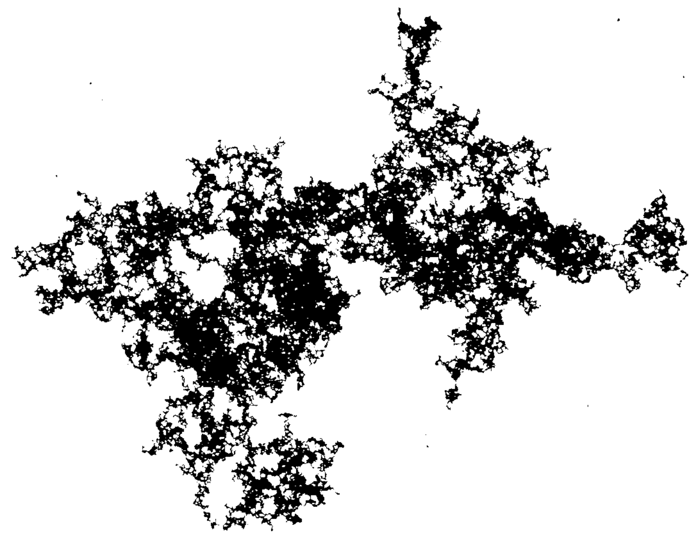

Fig. 1. An aggregate of 100-Å gold particles formed irreversibly in colloidal suspension. [Courtesy of M. Y. Lin and D. A. Weitz, Exxon Research and Engineering Co.]

Questions concerning these intersection probabilities are readily answered in terms of the fractal dimension. Let us define the mean number of intersections M_{12} (R) between two fractals 1 and 2, each of which has a radius of R and each of which is placed independently of the other in the same region of space. Then it can be shown (*23*) that

$$M_{12} \sim R^{D_1+D_2-d} \tag{3}$$

If the power of R is negative, the probability of intersection decreases indefinitely as the size R of the fractals increases. (This is possible because a very large fractal consists almost entirely of empty space.) Thus, in three dimensions, a light ray ($D_2 = 1$) almost always emerges from a sufficiently large aggregate, provided this aggregate has a fractal dimension of $D_1 < 2$. In this case the two structures are "mutually transparent."

On the other hand, a random walker ($D_2 = 2$) will escape from a very large fractal (in three dimensions) only if the large fractal has a dimension D_1 less than unity; this is impossible for a connected aggregate. Thus a random walk trajectory and an aggregate are "mutually opaque" in three dimensions. Similarly, a diffusing particle approaching an absorbing fractal of $D > d - 2$ from the exterior is almost always absorbed; the concentration of a solution of such particles is strongly depleted in the interior of the region spanned by the fractal. This result is surprisingly powerful when stated in more mathematical terms. In the space around an absorbing fractal of size R, the local concentration $u(r)$ obeys the steady-state diffusion (Laplace) equation

$$\nabla^2 u(r) = 0 \tag{4}$$

The boundary conditions are $u = 0$ on the fractal itself, and $u = u_\infty$, a constant, at infinity. Since u is strongly depleted in the interior region, the external field is similar to that of a perfectly absorbing sphere with a radius of about R.

Similar principles apply to the description of the hydrodynamic interactions of a fractal. In this case, the velocity $v(r)$ of a fluid

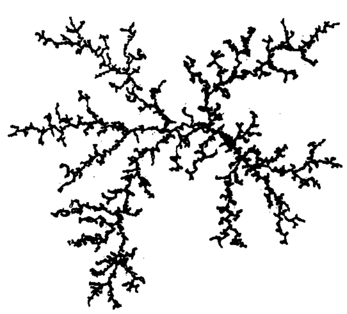

Fig. 2. Viscous fingering pattern formed when air displaces liquid epoxy in a two-dimensional porous medium (a monolayer of packed glass spheres sandwiched between glass plates). [From (*9*), courtesy of the American Physical Society]

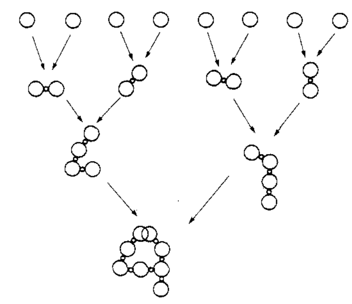

Fig. 3. Schematic of a hierarchical aggregation process. (Note the overlap of particles in the final cluster, which is permitted in the ghost model.)

moving at a low flow rate (low Reynolds number) in the vicinity of a suspended aggregate obeys a law that is like Eq. 4 and that has similar boundary conditions. The fractal absorbs the momentum of the fluid and strongly depletes the flow throughout the interior. The exterior velocity profile is like the flow around a hard sphere with a radius of about R. Thus the fractal diffuses, sediments, and increases the overall viscosity of a fluid as though the fractal were a hard sphere.

The concept of opacity may be used to treat the thermodynamics of a solution of aggregates. [A suitable solution can be made by stopping the gold aggregation process described in (*1*) in midcourse.] Two fractals are opaque to each other when they have $D > d/2$ (as seen from Eq. 3 with D_1 and D_2 equal to D). In this case, the osmotic pressure of a dilute solution of these aggregates in contact with a semipermeable membrane is comparable to what it would be if these were solid spheres of radius R. This result arises because configurations in which mutually opaque fractals interpenetrate significantly are rare.

Thus, to a considerable extent, a fractal aggregate interacts with external fields as though it were a solid object. This applies even though the average density within a large fractal of $D < d$ may be arbitrarily small. (Of course, such a fractal cannot behave like a solid object in every respect. For example, by increasing the concentration, a solution of mutually opaque aggregates can be forced to interpenetrate strongly, unlike a real solution of hard spheres.)

Aggregation Cluster by Cluster

At any stage during the colloidal aggregation process that leads to the cluster of Fig. 1, a typical collision is between two clusters of comparable size. The aggregation occurs "cluster by cluster." The final structure of the aggregates depends on the microscopic phenomena that control an individual aggregation event between two clusters. One possibility is that the rate-limiting step in the process is the diffusive approach of the two clusters before collision. This condition will hold for colloidal systems in which the aggregates move predominantly by Brownian motion and stick immediately and irreversibly to one another on first contact. Another possibility is that the clusters approach one another along straight-line (ballistic) trajectories, but still stick with certainty on contact. This mechanism occurs for aggregation in a vacuum or in colloidal systems under strong sedimentation. A third possibility is that the rate-limiting step is not the diffusive or ballistic approach of the clusters, but a local reaction governing the sticking event itself. In this reaction-limited regime, when two clusters collide, there is only a small probability that they will stick together.

In all three of the above cases, a more detailed analysis of the aggregation kinetics confirms that at each stage in the process the typical collision is between two clusters of roughly comparable size (*47–53*). A simple, solvable model embodying this idea is the "hierarchical ghost" model of Ball (*28*). In this model, pairs of single particles are linked to form dimers oriented in all directions. A pair of these dimers is selected at random and a particle of each is linked at random. In this way an ensemble of four-particle clusters is made. Then arbitrary pairs of these clusters are linked to make an ensemble of eight-particle clusters, and so forth (Fig. 3). This prescription preserves the treelike connectivity seen in real aggregates. One important interaction is omitted, however; at every stage, the constituent particles of a cluster are allowed to overlap in space. If these particles are solid, this is unrealistic. We discuss later the role of this neglected "excluded volume" effect.

The fractal dimension relating the mass of an aggregate to its radius is easy to calculate in this model (*28*). We define q_N as the average number of bonds along the connecting pathway between two particles on an N-particle cluster. From this q_N we can find the corresponding average q_{2N} for a $2N$-particle cluster made from two N-particle clusters, A and B. For two particles chosen at random on the $2N$-cluster there is a 25% chance that they both belong to the A cluster and a 25% chance that they both belong to the B cluster; in either case, the average distance is q_N. A 50% chance remains that one of the chosen particles belongs to A and the other to B. Clearly, the junction point between the two subclusters is itself a randomly chosen point on cluster A and cluster B. Hence the average number of bonds from each chosen particle to this point is q_N. Therefore, in this third case the average number of bonds between the two particles is $2q_N$. Taking the three cases together, one finds $q_{2N} = 3/2\ q_N$. Thus $q_N \sim N^{\log(3/2)/\log(2)}$. Since all sequences of bonds are random walks ($\delta = 2$), the average radius R of a cluster of N particles obeys $R \sim q_N^{1/2}$. Hence $N \sim R^{D_g}$, where $D_g = 2\log(2)/\log(3/2) \cong 3.4$ (*28*).

The main flaw in the hierarchical ghost model is neglect of the excluded volume effect. To account for this, we may modify the model as follows. The two subclusters are linked as before, but the combined cluster is then examined for pairs of overlapping particles. If there are any of these pairs, the cluster is discarded. This version of the model (*54*) describes the reaction-limited aggregation of equal-mass clusters. The importance of the excluded volume effect can be understood by again applying the concept of opacity described after Eq. 3. The excluded volume interaction of two clusters of fractal dimension D is statistically important only if they are mutually opaque, that is, if $D > d/2$. If, instead, the clusters are mutually transparent ($D < d/2$), then, even if constrained to touch at a point, they are unlikely to have a significant number of overlapping particles. This means that the neglect of the excluded volume effect is justifiable, and the ghost model is essentially correct, for space dimensions $d > 2D_g \cong 6.8$, but not for $d < 2D_g$.

Other variants of the hierarchical model describe growth of diffusing (*55*) or of ballistically moving (*18, 56*) clusters (in each case with immediate sticking on contact). In the diffusive version, the two clusters are chosen, placed at a large distance, and allowed to diffuse until they touch (*55*). They are then stuck permanently

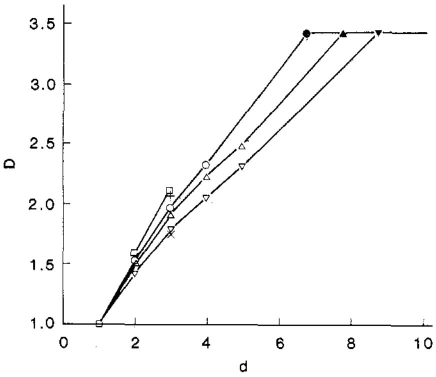

Fig. 4. Results for the fractal dimension D of cluster-cluster aggregates, as given by computer simulation on hierarchical models: reaction-limited (○), ballistic (△), and diffusive (▽) (*54–56, 59*). In each case the solid symbol is the exact result in high space dimensions (*28*). Squares denote nonhierarchical computer simulations in the reaction-limited regime (*58*). Nonhierarchical results for the ballistic (*57*) and diffusive (*31, 32, 57*) cases, in two and three dimensions, lie very close to the corresponding hierarchical values. Experimental data for diffusing and reaction-limited clusters in three dimensions are denoted by × and +, respectively (*1, 34*).

together by a rigid bond. Equivalently, one may choose one particle on each subcluster and link these to form the aggregate, as in the ghost model. But then one of the subclusters is detached and made to execute a random walk to infinity. If the two subclusters intersect at any time during this walk, the combined cluster is discarded. The opacity argument now applies to one subcluster and the path swept out by the other. This path is an object constructed by replacing every site of that subcluster by a random walk; such an object has a fractal dimension equal to that of the subcluster plus two. For this process then, the ghost approximation is justified for $d > 2D_g + 2 \cong 8.8$. The corresponding criterion in the ballistic case is $d > 2D_g + 1 \cong 7.8$ (*28*).

In two and three dimensions—far from the high space dimensions in which the ghost model is valid—we expect the excluded volume effect to play a major role. When two N-site clusters are joined together, the resulting $2N$-cluster will almost surely be discarded unless the junction point is near the periphery of both subclusters. Hence the size R of the combined cluster is on average larger than in the ghost model. Doubling the mass thus increases the size by a larger factor than before; accordingly, D is smaller than D_g. The reduction in D is most marked for the diffusion-limited case: two clusters approaching one another with random-walk trajectories are likely to make their first contact at a point that is very near an exposed tip on each of the clusters. If the approach is ballistic, it is more likely that partial interpenetration will occur before sticking. For reaction-limited aggregation this is even more likely, and the reduction in D should be the least for this case. Also, since the excluded volume effect is small for high space dimensions, the fractal dimension D of an aggregate made by any given mechanism should increase with the space dimension d in which it was made. These trends are confirmed by computer simulations and experiments (Fig. 4). Values of D lie between 1.4 and 1.6 in two dimensions, and between 1.6 and 2.2 in three.

A defect of the hierarchical models so far discussed is the assumption that colliding clusters have exactly equal mass. In reality, the reacting masses are taken from a certain statistical distribution, which can be calculated in detail by studying the kinetic equations governing the aggregation process (*47–53*). This effect can be accounted for in a ghost model (*29*); it is found to increase the fractal dimension of the clusters somewhat (from 3.4 to about 3.7). For lower space dimension one also expects an increase in D, since, even when the excluded volume effect is strong, a small cluster can penetrate into the gaps in a bigger cluster before a sticking event occurs. However, the difference in D seems to be a measurable one only in the reaction-limited case (*57–59*).

Another effect omitted throughout the above discussion is the annealing of the aggregate during its formation. As aggregation proceeds, the clusters eventually become so large that they start to flex significantly as a result of random thermal motion. At this time the arms of any given cluster are likely to come into contact; when they do so, they will stick. After a longer time, the resulting aggregates should be treelike at short distances, but should form a relatively well-connected weblike network, with increased D, at larger distances. A second annealing mechanism is the local rearrangement of material at short length scales. This can cause a slow evolution of the cluster toward a state of lowest free energy. (If the particles attract one another, this is a compact clump with $D = d$.) These annealing effects may be important in many real aggregates.

Aggregation Particle by Particle

We now discuss clusters that are formed by the aggregation of particles one at a time. These processes can be classified according to how an incoming particle moves to join the cluster. The case where it does not move, but simply materializes at a random unoccupied site adjacent to the existing cluster, is known as the Eden model (*60*). The resulting structure has a rather uniform density, with a fractal dimension $D = d$, characteristic of a space-filling object (*32, 61*). The same is true for ballistically moving particles (*18, 62, 63*).

If, on the other hand, each particle executes a random walk to join the aggregate, a tenuous fractal structure of $D < d$ results (Fig. 5) (*32, 33*). This diffusion-limited aggregation model (DLA) has been extensively studied by computer simulation. Values of the fractal dimension are $D = 1.7$ and $D = 2.5$ in two and three dimensions, respectively. The DLA model is the more interesting because of its relation to several random growth phenomena in nature. All these growth mechanisms are controlled by Laplacian fields.

In DLA, the probability of growth at a given perimeter site next to the cluster is the probability that a random walker, starting at some point far from the cluster, visits this site before visiting any other perimeter site. The probability $u(r)$ that the incoming particle is at point r obeys the steady-state diffusion equation (Eq. 4), where u is some constant at infinity and is zero on the perimeter sites. The probability of adsorption onto a given perimeter site is proportional to the field u adjacent to that site. The relative rates of growth are thus controlled by a Laplacian field. The same equation is obeyed in two-fluid flow in a porous medium (*6*), when a low-viscosity fluid is pumped into a region occupied by high-viscosity fluid. The Laplacian field is the pressure; its gradient (times a mobility coefficient) is the local flow velocity. The fluid-fluid interface displays a viscous fingering instability (*64*). When the difference in viscosities is very large, such flow can lead to a tenuous fractal interface with scaling properties similar to those of DLA (compare Fig. 2 with Fig. 5) (*7–9*).

Diffusion-limited solidification is another phenomenon of the same type (*10, 65*). Here the diffusing field may be heat or a chemical species; the local growth rate is proportional to the flux of this field. Experiments show that this process can also lead to a tenuous structure with fractal behavior consistent with two- or three-dimensional DLA (*11, 12*). Finally, the electrical breakdown of an insulating medium is controlled by the (Laplacian) electrostatic potential (*14, 32*). The connection with the DLA model is here less direct, however, since the growth rate need not depend linearly on the gradient of the field. Despite this, the patterns formed in breakdown bear a striking qualitative resemblance to DLA (*14*).

Although DLA clusters share certain morphological features with those arising in cluster-by-cluster aggregation (such as the absence of loops), there are nonetheless several important differences. For

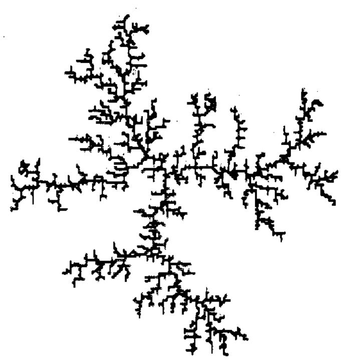

Fig. 5. Computer-generated picture of a DLA cluster grown in two dimensions. [From (*32*), courtesy of the American Physical Society]

example, the length $L(r)$ of a connecting path seems to be proportional to the geometric distance r (that is, $\delta = 1$) in all space dimensions (*66*). A systematic theoretical understanding of this and other features of the DLA structure is lacking. One reason for this lack of understanding is that a simple description of DLA in high-dimensional space has not been discovered. Rather, it has been shown (*63, 67*) that in all space dimensions d, the fractal dimension obeys $D \geq d - 1$. This behavior contrasts with cluster-by-cluster aggregation in which D attains a finite limiting value in high space dimensions.

Despite these difficulties, it is possible to get some qualitative feel for the highly ramified structure of a DLA cluster from a more detailed consideration of the growth process. First, each part of the fractal is opaque to the diffusing field, so if some branch of the cluster grows slightly ahead of its neighbors, that branch tends to catch all the incoming particles and causes the neighboring limbs to fall farther behind. This instability leads to fingerlike growth, in which most of the incoming particles land near the outermost tips of the cluster (*68*). A second ingredient in the DLA growth pattern is the presence of microscopic noise or randomness. In the case of aggregation or deposition, the noise is inherent in the discrete randomness of the incoming particles. In the case of viscous fingering or dielectric breakdown, the noise arises because of disorder in the underlying porous material or insulator. The noise causes branching at the tips of the growing structure. The newly formed branches compete for incoming particles as outlined above; thus there is always a dynamic balance between branching events at the local level and the gradual eclipse of most branches in the competition for the incoming particles.

These balancing effects can be varied in several interesting ways to produce structures related to ordinary DLA. First, one can introduce a "surface tension," which inhibits fingering and tends to damp out fluctuations in the density of incoming particles. This process is equivalent to allowing some particles to reevaporate from the cluster after deposition and diffuse to a new site (*69*). It thus may be thought of as an annealing effect. Second, the large-scale shape of DLA clusters is unexpectedly sensitive to various forms of anisotropy. For example, clusters grown on a square lattice develop an overall crosslike shape that becomes more and more pronounced as the size increases (*70–73*). DLA also appears to be unstable with respect to anisotropy in the microscopic laws governing the sticking of particles to the cluster (*72*).

Conclusions

In this article we have given an overview of recent advances in the understanding of fractal aggregates. Inevitably, much important work has not been discussed. For example, in the field of cluster-by-cluster aggregation, progress has been made toward developing a detailed understanding of aggregation kinetics, which has led to predictions of the cluster size distribution and its dynamical evolution under various conditions (*48–53*). We have not discussed work on colloidal aggregation at high concentrations or the related phenomenon of kinetic gelation (*19–22*). While progress continues in these areas, it seems that the basic ideas underlying cluster-by-cluster aggregation are qualitatively understood.

In contrast, our understanding of particle-by-particle aggregation is comparatively incomplete. Although progress has been made with the Eden model (*74–76*) and in the ballistic case (*63, 77*), results have been unsatisfactory in the case of DLA (and related processes) where growth is controlled by diffusing particles or fields. Here we lack even a schematic model to show why this type of growth leads to a scale-invariant structure. Furthermore, DLA shows surprising anisotropy effects and sensitivity to noise that have not yet been explained. The solutions to these puzzles may hold the key to understanding a wide class of natural phenomena that produce the distinctive ramified patterns of DLA. Further progress in the understanding of DLA may also elucidate other irreversible processes involving the interaction of large numbers of particles.

REFERENCES AND NOTES

1. D. A. Weitz, J. S. Huang, M. Y. Lin, J. Sung, *Phys. Rev. Lett.* **54**, 1416 (1985); D. A. Weitz and M. Oliveria, *ibid.* **52**, 1433 (1984).
2. D. C. Sieglia and G. W. Smith, Eds., *Particulate Carbon Formation During Combustion* (Plenum, New York, 1981).
3. J. B. Donnet and A. Voet, *Carbon Black Physics Chemistry and Elastomer Reinforcement* (Dekker, New York, 1976).
4. J. Eisenlauer and E. Killmann, *J. Colloid Interface Sci.* **74**, 108 (1980).
5. J. Y. Bottero, J. M. Cases, F. Fiessinger, J. E. Poivier, *J. Phys. Chem.* **84**, 2933 (1980).
6. L. Paterson, *Phys. Rev. Lett.* **52**, 1625 (1984).
7. J. Nittman, G. Daccord, H. E. Stanley, *Nature (London)* **314**, 141 (1985).
8. R. Lenormand and C. Zarcone, *Phys. Rev. Lett.* **54**, 2226 (1985); J. D. Chen and D. Wilkinson, *ibid.* **55**, 1892 (1985).
9. K. J. Maloy, J. Feder, T. Jossang, *ibid.* **55**, 2688 (1985).
10. J. S. Langer, *Rev. Mod. Phys.* **52**, 1 (1980).
11. R. M. Brady and R. C. Ball, *Nature (London)* **309**, 225 (1984).
12. E. Ben-Jacob *et al.*, *Phys. Rev. Lett.* **55**, 1315 (1985).
13. M. Matsushita, M. Sano, Y. Hakayawa, H. Honjo, Y. Sawada, *ibid.* **53**, 286 (1984).
14. L. Niemeyer, L. Pietronero, H. J. Wiessmann, *ibid.* **52**, 1033 (1984).
15. K. Kusaka, N. Wada, A. Tasaki, *J. Appl. Phys.* **8**, 599 (1969); A. I. Medalia, *Rubber Chem. Technol.* **51**, 437 (1978).
16. S. K. Friedlander, *Smoke, Dust, and Haze* (Wiley, New York, 1977); Faraday Symposium 7, *Fogs and Smokes* (Faraday Division, Chemical Society, London, 1973).
17. D. N. Sutherland and I. Goodard-Nia, *Chem. Eng. Sci.* **26**, 2071 (1971); D. N. Sutherland, *Nature (London)* **226**, 1241 (1970).
18. M. J. Vold, *J. Colloid Sci.* **18**, 684 (1963); *J. Phys. Chem.* **63**, 1608 (1959); D. N. Sutherland, *J. Colloid Interface Sci.* **25**, 373 (1967).
19. F. Family and D. P. Landau, Eds., *Kinetics of Aggregation and Gelation* (Elsevier, Amsterdam, 1984).
20. N. Boccara and M. Daoud, Eds., *Physics of Finely Divided Matter* (Springer-Verlag, Berlin, 1985).
21. N. Ostrowsky and H. E. Stanley, Eds., *On Growth and Form, a Modern View* (Nijhoff, The Hague, 1985).
22. R. Pynn and A. Skjeltorp, Eds., *Scaling Phenomena in Disordered Systems* (Plenum, New York, 1985); L. Pietronero, Ed., *Fractals in Physics* (Elsevier, Amsterdam, 1985).
23. B. B. Mandelbrot, *The Fractal Geometry of Nature* (Freeman, San Francisco, 1982).
24. P. G. de Gennes, *Scaling Concepts in Polymer Physics* (Cornell Univ. Press, Ithaca, NY, 1979).
25. B. Zimm and W. Stockmayer, *J. Chem. Phys.* **17**, 301 (1949).
26. T. C. Lubensky and J. Isaacson, *Phys. Rev. A* **20**, 2130 (1979).
27. J. Isaacson and T. C. Lubensky, *J. Phys. (Paris) Lett.* **41**, L469 (1980).
28. R. C. Ball and T. A. Witten, *J. Stat. Phys.* **36**, 863 (1984).
29. R. C. Ball, *Physica B* **127**, 87 (1984).
30. P. Meakin, *Phys. Rev. Lett.* **51**, 1119 (1983).
31. M. Kolb, R. Botet, R. Jullien, *ibid.*, p. 1123.
32. T. A. Witten and L. M. Sander, *ibid.* **47**, 1400 (1981); *Phys. Rev. B* **27**, 5686 (1983).
33. P. Meakin, *Phys. Rev. A* **27**, 1495 (1983).
34. D. W. Schaefer, J. E. Martin, P. Wiltzius, D. S. Cannell, *Phys. Rev. Lett.* **52**, 2371 (1984).
35. S. R. Forrest and T. A. Witten, *J. Phys. A* **12**, L109 (1979).
36. A. J. Hurd and D. W. Schaefer, *Phys. Rev. Lett.* **54**, 1043 (1985).
37. C. Allain and B. Jouhier, *J. Phys. (Paris) Lett.* **44**, L421 (1983); P. Richetti, J. Prost, D. Barois, *ibid.* **45**, L1137 (1984); C. Camoin and R. Blanc, *ibid.* **46**, L67 (1985).
38. S. Alexander and R. Orbach, *ibid.* **43**, L625 (1982).

39. R. Rammal and G. Toulouse, *ibid.* **44**, L13 (1983).
40. S. Havlin, Z. Djordjevic, I. Majid, H. E. Stanley, G. H. Weiss, *Phys. Rev. Lett.* **53**, 178 (1984).
41. F. Family and A. Coniglio, *J. Phys. A* **17**, L285 (1984).
42. M. E. Cates, *ibid.*, p. L489.
43. Y. Kantor and I. Webman, *Phys. Rev. Lett.* **52**, 1891 (1984).
44. Y. Kantor and T. A. Witten, *J. Phys. (Paris) Lett.* **45**, L675 (1984).
45. I. Webman, in *Physics of Finely Divided Matter*, N. Boccara and M. Daoud, Eds. (Springer-Verlag, Berlin, 1985), pp. 180–187.
46. M. E. Cates, *Phys. Rev. Lett.* **53**, 926 (1984).
47. M. V. von Smoluchowski, *Z. Phys.* **17**, 557 (1916).
48. R. M. Ziff, *J. Stat. Phys.* **23**, 241 (1980).
49. M. H. Ernst, E. M. Hendriks, F. Leyvraz, *J. Phys. A* **17**, 2137 (1984).
50. F. Leyvraz and H. R. Tschudi, *ibid.* **15**, 1951 (1982).
51. R. M. Ziff, E. M. Hendriks, M. H. Ernst, *Phys. Rev. Lett.* **49**, 593 (1982).
52. T. Vicsek and F. Family, *ibid.* **52**, 1669 (1984).
53. R. Botet and R. Jullien, *J. Phys. A* **17**, 2517 (1984).
54. R. Jullien and M. Kolb, *ibid.*, p. L639.
55. ______, R. Botet, *J. Phys. (Paris) Lett.* **45**, L211 (1984).
56. R. Jullien, *J. Phys. A* **17**, L771 (1984).
57. P. Meakin, *Phys. Rev. A* **29**, 997 (1984).
58. W. D. Brown and R. C. Ball, *J. Phys. A* **18**, L517 (1984).
59. R. C. Ball and R. Jullien, *J. Phys. (Paris) Lett.* **45**, L103 (1984).
60. M. Eden, in *Proceedings of the Fourth Berkeley Symposium on Mathematical Statistics and Probability*, J. Neyman, Ed. (Univ. of California Press, Berkeley, 1961).
61. H. Peters, D. Stauffer, H. P. Holters, K. Loewemich, *Z. Phys.* **B34**, 399 (1979).
62. D. Bensimon, B. Shraiman, S. Liang, *Phys. Lett.* **102A**, 238 (1984).
63. R. C. Ball and T. A. Witten, *Phys. Rev. A* **29**, 2966 (1984).
64. P. G. Saffman and G. I. Taylor, *Proc. R. Soc. London Ser. A* **245**, 312 (1958).
65. J. S. Langer and H. Mueller-Krumbhaar, *Acta Metall.* **2**, 1081 (1978); *ibid.*, p. 1689.
66. P. Meakin, I. Majid, S. Havlin, H. E. Stanley, *J. Phys. A* **17**, L975 (1984).
67. R. C. Ball, M. Nauenberg, T. A. Witten, *Phys. Rev. A* **29**, 2017 (1984).
68. P. Meakin and T. A. Witten, *ibid.* **28**, 2985 (1983).
69. L. P. Kadanoff, *J. Stat. Phys.* **39**, 267 (1985).
70. R. C. Ball and R. M. Brady, *J. Phys. A* **18**, L809 (1985).
71. P. Meakin, *Phys. Rev. A* **33**, 3371 (1986).
72. R. C. Ball, R. M. Brady, G. Rossi, B. R. Thompson, *Phys. Rev. Lett.* **55**, 1906 (1985).
73. L. A. Turkevich and H. Sher, *ibid.*, p. 415.
74. G. Parisi and Y. C. Zhang, *ibid.* **53**, 1791 (1984).
75. D. Dhar and R. Ramaswamy, *ibid.* **54**, 1346 (1985); D. Dhar, *ibid.*, p. 2058.
76. J. Vannimenus, B. Nickel, V. Hakim, *Phys. Rev. B* **30**, 391 (1984); R. M. Bradley and P. N. Strenski, *ibid.* **31**, 4319 (1985).
77. S. Liang and L. P. Kadanoff, *Phys. Rev. A* **31**, 2628 (1985); P. Ramanlal and L. M. Sander, *Phys. Rev. Lett.* **54**, 1828 (1985).

Mechanisms of Memory

LARRY R. SQUIRE

Recent studies of animals with complex nervous systems, including humans and other primates, have improved our understanding of how the brain accomplishes learning and memory. Major themes of recent work include the locus of memory storage, the taxonomy of memory, the distinction between declarative and procedural knowledge, and the question of how memory changes with time, that is, the concepts of forgetting and consolidation. An important recent advance is the development of an animal model of human amnesia in the monkey. The animal model, together with newly available neuropathological information from a well-studied human patient, has permitted the identification of brain structures and connections involved in memory functions.

MOST SPECIES ARE ABLE TO ADAPT IN THE FACE OF EVENTS that occur during an individual lifetime. Experiences modify the nervous system, and as a result animals can learn and remember. One powerful strategy for understanding memory has been to study the molecular and cellular biology of plasticity in individual neurons and their synapses, where the changes that represent stored memory must ultimately be recorded (*1*). Indeed, behavioral experience directly modifies neuronal and synaptic morphology (*2*). Of course, the problem of memory involves not only the important issue of how synapses change, but also questions about the organization of memory in the brain. Where is memory stored? Is there one kind of memory or are there many? What brain processes or systems are involved in memory and what jobs do they do? In recent years, studies of complex vertebrate nervous systems, including studies in humans and other primates, have begun to answer these questions.

The author is a research career scientist at the San Diego Veterans Administration Medical Center, San Diego, CA 92161, and a professor of psychiatry, University of California School of Medicine, La Jolla, CA 92093.

Memory Storage: Distributed or Localized?

The collection of neural changes representing memory is commonly known as the engram (*3*), and a major focus of contemporary work has been to identify and locate engrams in the brain. The brain is organized so that separate regions of neocortex simultaneously carry out computations on specific features or dimensions of the external world (for example, visual patterns, location, and movement). The view of memory that has emerged recently, although it still must be regarded as hypothesis, is that information storage is tied to the specific processing areas that are engaged during learning (*4, 5*). Memory is stored as changes in the same neural systems that ordinarily participate in perception, analysis, and processing of the information to be learned. For example, in the visual system, the inferotemporal cortex (area TE) is the last in a sequence of visual pattern-analyzing mechanisms that begins in the striate cortex (*6*). Cortical area TE has been proposed to be not only a higher order visual processing region, but also a repository of the visual memories that result from this processing (*4*).

The idea that information storage is localized in specific areas of the cortex differs from the well-known conclusion of Lashley's classic work (*7*) that memory is widely and equivalently distributed throughout large brain regions. In his most famous study, Lashley showed that, when rats relearned a maze problem after a cortical